nature communications

Article

https://doi.org/10.1038/s41467-026-69511-z

Sensory coding of borneol repellency in culicine mosquitoes via the *Or49* pathway

Received: 26 June 2024

Accepted: 2 February 2026

Published online: 20 February 2026

Check for updates

Yuri Vainer[1,8], Evyatar Sar-Shalom[1,8], Yinliang Wang[1,2,8], Robert M. Huff[3], Dor Perets[1], Esther Yakir[1], Majid Ghaninia[4], Iliano V. Coutinho-Abreu[5], Carlos Ruiz[6], Dhivya Rajamanickam[3], Alon Warburg[7], Omar S. Akbari[5], Philippos A. Papathanos[1], Rickard Ignell[4], Jeffrey A. Riffell[6], Ronald Jason Pitts[3] ✉ & Jonathan D. Bohbot[1] ✉

Plant-derived repellents containing borneol and camphor have been used for centuries, yet the sensory mechanisms that mediate their effects in mosquitoes have remained obscure. Here, we show that culicine mosquitoes possess a dedicated olfactory pathway for detecting bicyclic monoterpenoids. We identify odorant receptor 49 (OR49) as a conserved and highly selective borneol receptor expressed in a distinct neuron of the maxillary palp. This neuron forms a defined projection to the MD3 glomerulus in the antennal lobe, establishing a labeled line for plant-derived repellents. Genetic disruption of *Or49* abolishes electrophysiological responses to borneol and markedly diminishes avoidance behavior during human host-seeking. These results reveal that female mosquitoes detect borneol through a specialized sensory channel distinct from those mediating attraction to human cues. Our findings provide a mechanistic framework for understanding how plant volatiles shape mosquito behavior and offer a foundation for the rational design of next-generation olfactory repellents.

The use of plants to ward off insects has been a human practice since prehistoric times[1] and is still used in many parts of the world[2,3]. Plant-based essential oils (EOs), including lemon eucalyptus leaf oil[4], citronella oil[5], and coconut oil[6] exhibit different degrees of mosquito repellency due to the presence of pyrethrins[7], phenol derivatives, and terpenoids[8]. The latter includes oxygen-containing compounds with open-chain hydrocarbons, such as linalool, citronellol, geraniol, and bicyclic derivatives such as cineole, fenchone, camphor, and borneol (Fig. 1a). The EO of the camphor tree *Cinnamomum camphora* is composed of over 70 volatile organic compounds (VOCs), most of which are oxygenated monoterpenes dominated by camphor and other related compounds[9]. Camphor and borneol extracts are believed to have originated from the camphor tree in the island of Borneo (Fig. 1a), where they were initially traded with China and then introduced to the West due to their therapeutic, refreshing, and repellent effects against mosquitoes[10]. How these terpenoids molecules exert repelling effects against mosquitoes is not well-understood but is likely mediated by their olfactory system.

The capitate-peg (cp) sensillum located on the mosquito maxillary palp comprises three olfactory neurons, each distinguishable by size, olfactory receptor gene expression profile, and odor response characteristics (Fig. 1b). In both culicine and anopheline mosquitoes, the largest olfactory sensory neuron (cpA) expresses three gustatory receptors (*Grs*) that specifically detect CO_2[11,12]. The

[1]Department of Entomology, The Hebrew University of Jerusalem, Rehovot, Israel. [2]Agriculture Gene Engineering Research Center of the Ministry of Education, Northeast Normal University, Changchun, China. [3]Department of Biology, Baylor University, Waco, USA. [4]Department of Plant Protection Biology, Swedish University of Agricultural Sciences, Alnarp, Sweden. [5]School of Biological Sciences, Department of Cell and Developmental Biology, University of California San Diego, La Jolla, CA, USA. [6]Department of Biology, University of Washington, Seattle, WA, USA. [7]Department of Microbiology and Molecular Genetics, The Hebrew University of Jerusalem, Jerusalem, Israel. [8]These authors contributed equally: Yuri Vainer, Evyatar Sar-Shalom, Yinliang Wang. ✉e-mail: Jason_Pitts@baylor.edu; jonathan.bohbot@mail.huji.ac.il

https://doi.org/10.1038/s41467-026-69511-z

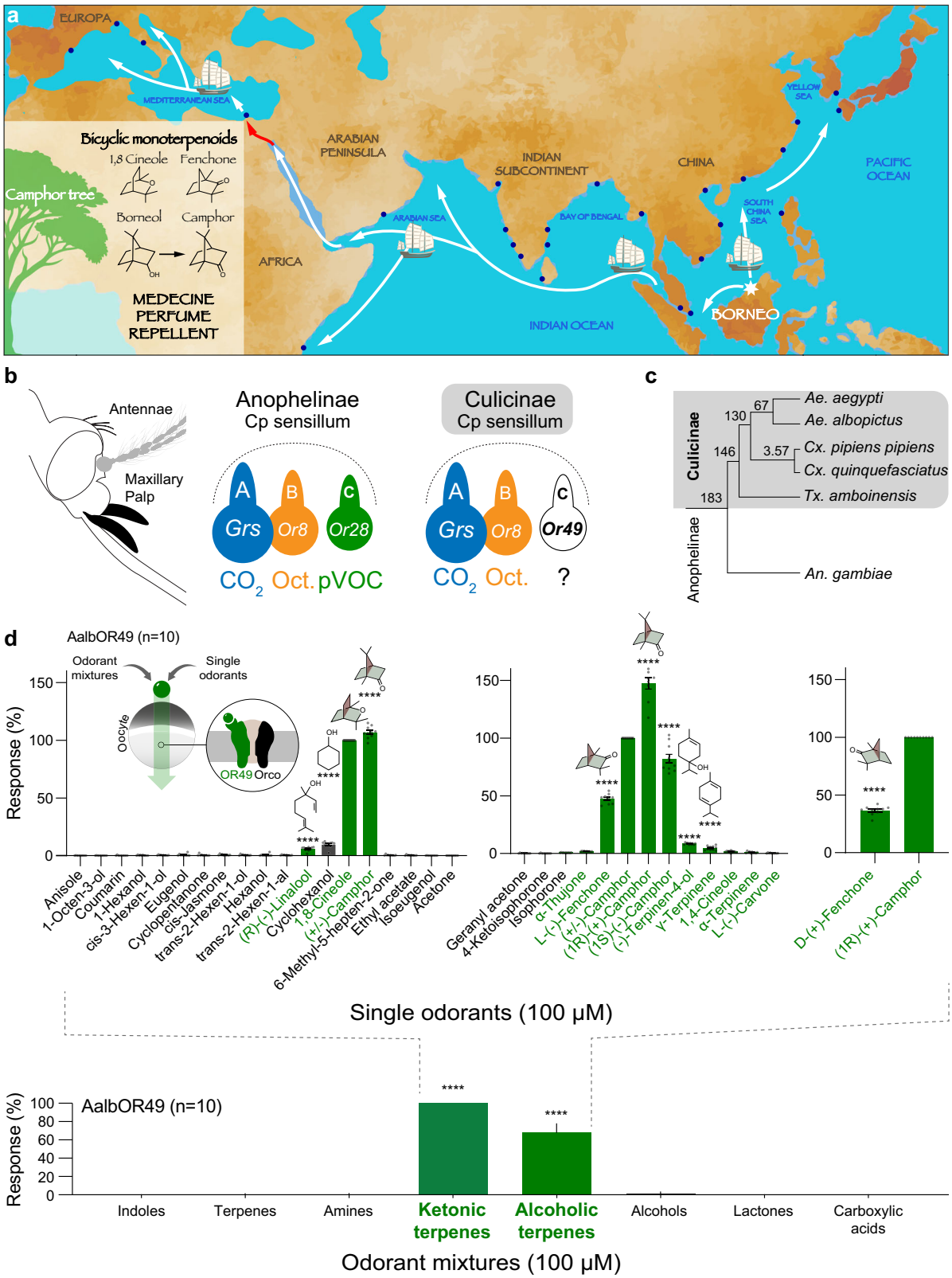

medium-sized cpB neuron of *Anopheles gambiae* and *Aedes aegypti* expresses the 1-octen-3-ol odorant receptor *Or8* and its co-receptor Orco[13–15]. Both CO_2 and 1-octen-3-ol elicit attraction and signal the presence of animal hosts in anopheline[16] and culicine[17] mosquitoes. This cellular and functional organization has remained remarkably conserved over 180 million years of mosquito evolution (Fig. 1c).

In anophelines, the small cpC neuron expresses the *Or28* gene[13], which responds to plant volatile organic compounds (pVOC)[18]. In culicines, the cpC neuron expresses the *Or49* gene[19], which is unrelated to *AgamOr28* (Fig. 1b). Using a pharmacological approach, we expressed *Or49* in a heterologous expression system and exposed it to odorant mixtures, EOs, and individual VOCs. Our findings provide strong evidence that the OR49 receptor and the cpC neuron respond

Fig. 1 | Odorant receptor 49 is activated by bicyclic monoterpenoids. a Borneol and camphor oils from the camphor tree *Cinnamomum camphora* originated from the island of Borneo and were traded with China and the rest of the Western world through the maritime silk road during the classical age due to their medicinal and repellent properties. The world map is adapted from an illustration available on Vecteezy.com (free license). Blue dots indicate major global trading ports. **b** The capitate peg sensillum (cp) on the 4th segment of the mosquito maxillary palps houses three neurons, including the CO_2-sensitive neuron (cpA) expressing three gustatory receptors, the 1-octen-3-ol-sensitive neuron (cpB) expressing *Or8*, and in Culicine mosquitoes, the orphan neuron (cpC) expressing *Or49*. **c** Phylogenetic relationship and assigned ontology across six mosquito species. Numbers indicate divergence times in millions of years. **d** Bottom - The response profile of *Aedes albopictus* OR49 (AalbOR49) to odorant mixtures (100 µM) belonging to a variety of chemical classes highlights the activity of ketonic and alcoholic terpenes. Top - Bicyclic monoterpenoids, including camphor and fenchone, are the most efficacious activators of AalbOR49 (labeled in green). Statistical differences were evaluated by Ordinary one-way ANOVA followed by a Holm-Sidak's multiple comparison test. ns, non-significant, $^{****}p < 0.0001$. Data are presented as mean values +/- SEM. Source data are provided as a Source Data file.

to plant-derived bicyclic monoterpenoids with a marked selectivity towards borneol, traditionally used as a mosquito repellent. To directly assess its olfactory function, we generated an *Or49* null mutant line in *Aedes aegypti*, which completely lacked electrophysiological responses to borneol and displayed reduced avoidance behavior in the context of human-host seeking. Furthermore, we show that borneol selectively activates the MD3 glomerulus in the antennal lobe of *Ae. aegypti*. Together, these results provide a framework for dissecting the molecular and neural mechanisms underlying olfactory integration and host-seeking behavior in mosquitoes.

Results

Odorant receptor 49 is an evolutionary conserved and selective borneol receptor

The odorant receptor 49 gene [19] is represented by conserved 1-to-1 orthologs in *Aedes albopictus*, *Culex quinquefasciatus, Toxorhynchites amboinensis,* and *Aedes aegypti* (Supplementary Fig. 1). Phylogenetic analyses support previous studies[19,20] describing the OR49 family as Culicinae-specific with no conserved orthologs detected in *Anopheles* (Supplementary Fig. 1c–d). However, related *Or49*-like genes are located on chromosome 2 in both *Aedes* and *Anopheles* mosquitoes (Supplementary Fig. 1e). Clear evidence of conserved synteny with neighboring genes is observed between *Ae. aegypti* and *Ae. albopictus* (Supplementary Fig. 1e–f).

As a continuation of our work on the functional identity of the cp sensillum in culicine mosquitoes[19,21], we investigated the receptive field of *Ae. albopictus* OR49 (AalbOR49) using two-electrode voltage clamp recordings (Fig. 1d) and a panel of 81 odorants representing diverse chemical classes (Supplementary Data 1). *Xenopus laevis* oocytes expressing functional receptor complexes were strongly activated by blends containing ketonic and alcoholic terpenes (Fig. 1d bottom). Testing of single compounds from these two active blends revealed the efficacy of bicyclic monoterpenoids. (1R)-(+)-camphor emerged as the most efficacious ligand, followed by 1,8-cineole (also called eucalyptol) and both stereoisomers of fenchone (Fig. 1d).

In an independent set of experiments, we investigated the potential of *Cannabis* EOs (Supplementary Fig. 2, Supplementary Data 1) to activate OR49 from the nectar-feeding species *Tx. amboinensis* (TambOR49) (Fig. 2a-b). We tested eight *Cannabis* EOs (Fig. 2c) containing a total of 42 plant VOCs, dominated by terpenes (Supplementary Fig. 2). Among these, the most active were Pineapple Haze, OG Kush, and Adom #9, while Master Kush and Jack Herrer showed much lower efficacy. Furthermore, Alien OG, Forbidden Fruit and Kush Note did not activate the receptor (Fig. 2c). All active mixtures evoked consistent current responses (Supplementary Fig. 3). Successive fractionations of these EOs into 6 sub-mixtures and 4 single compounds revealed that racemic borneol is the most potent compound (Fig. 2d), consistent with its content in the original *Cannabis* mixtures (Fig. 2c, Supplementary Fig. 4a) and sub-mixtures (Supplementary Fig. 4b). TambOR49 and AaegOR49 did not exhibit enantioselectivity towards the (+) and (−)-borneol enantiomers (Fig. 2e), as indicated by their EC_{50} values in the one-digit micromolar range. We therefore focused subsequent oocyte analyses on the (+) enantiomers. OR49 orthologs from *Ae. albopictus*, *Ae. aegypti*, *Cx. quinquesfasciatus* and *Tx. amboinensis* all responded robustly to the two most potent ligands, (+)-borneol and (+)-camphor, although with varying selectivity. We established concentration-response relationships with these ligands in TambOR49, *Cx. quinquefasciatus* OR38 (CquiOR38), *Ae. aegypti* OR49 (AaegOR49), and *Ae. allbopictus* OR49 (AalbOR49) (Fig. 2f). (+)-Borneol was 19-32 times more potent than (+)-camphor in all cases except for TambOR49 where both compounds were equally active in the low micromolar range (Fig. 2f). However, when comparing maximum response magnitudes, (+)-borneol consistently elicited higher currents than (+)-camphor across all four culicine species, including the nectar-feeding *Tx. amboinensis* (Fig. 2g, Supplementary Fig. 3). These results indicate that OR49 shows strong selectivity for borneol and closely related compounds.

By contrast, in *An. gambiae*, the cpC neuron expresses OR28 instead of OR49 (Fig. 1b). This receptor is activated by plant VOCs, with acetophenone and 2,4,5-trimethylthiazole being the most effective ligands in the *Xenopus* oocyte expression system[13,18]. The EC_{50} values of acetophenone, α-pinene, and α-terpineol were in the low millimolar range, indicating that more potent ligands remain to be identified (Supplementary Fig. 5). Notably, borneol did not elicit any response at the tested concentrations suggesting that AgamOR28 is tuned to VOCs belonging to a different chemical class.

The *Or49* gene confers sensitivity to borneol

To investigate the olfactory effect of camphor and borneol in vivo, we conducted electropalpogram (EPG) recordings on three culicine (*Ae. albopictus*, *Ae. aegypti*, *Cx. pipiens*) and one anopheline (*An. gambiae*) species (Fig. 3a). 1-Octen-3-ol, which served as a positive control, induced significant responses in all mosquitoes tested. Camphor and borneol elicited consistent palp responses in Culicine mosquitoes, including *Ae. albopictus*, *Ae. aegypti*, and *Cx. pipiens* but not in *An. gambiae*, which expresses *Or28* in the palp instead of *Or49* (Fig. 3b). Camphor and borneol evoked lower responses than 1-octen-3-ol in the culicine palps. In *Ae. albopictus*, (−)-borneol was more active than (+)-camphor, while in *Ae. aegypti* both borneol enantiomers elicited significantly greater EPG responses than camphor enantiomers. In *Cx. pipiens*, borneol and camphor elicited comparable EPG responses. We established dose-response relationships with (+)-camphor and (+)-borneol in *Ae. albopictus*, *Ae. aegypti*, and *Cx. pipiens* (Fig. 3c). Aedine spp. exhibited significantly larger responses to (+)-borneol in doses higher than 0.1 µg. While *Cx. pipiens* exhibited statistically significant larger responses in response to (+)-camphor in doses higher than 1 µg.

To test a potential causal relationship between *Or49* and the borneol response, we used CRISPR-Cas9 to knock out the *Or49* gene in *Ae. aegypti*, which serves as a more genetically tractable model than *Ae. albopictus* (Supplementary Fig. 6). This knockout line exhibits a 442 bp deletion spanning the start codon and the first exon of the *Or49* gene, along with multiple SNPs upstream at the promoter sequence (Supplementary Fig. 6).

To investigate the genetic mechanism determining borneol sensitivity in the palp, we conducted single-sensillum recordings (Fig. 4a) from the cp sensillum of *Ae. aegypti* (Fig. 4c), *An. gambiae* (Fig. 4d), *Ae. albopictus* (Fig. 4e), and *Cx. quinquefasciatus* (Fig. 4f). The response of

https://doi.org/10.1038/s41467-026-69511-z

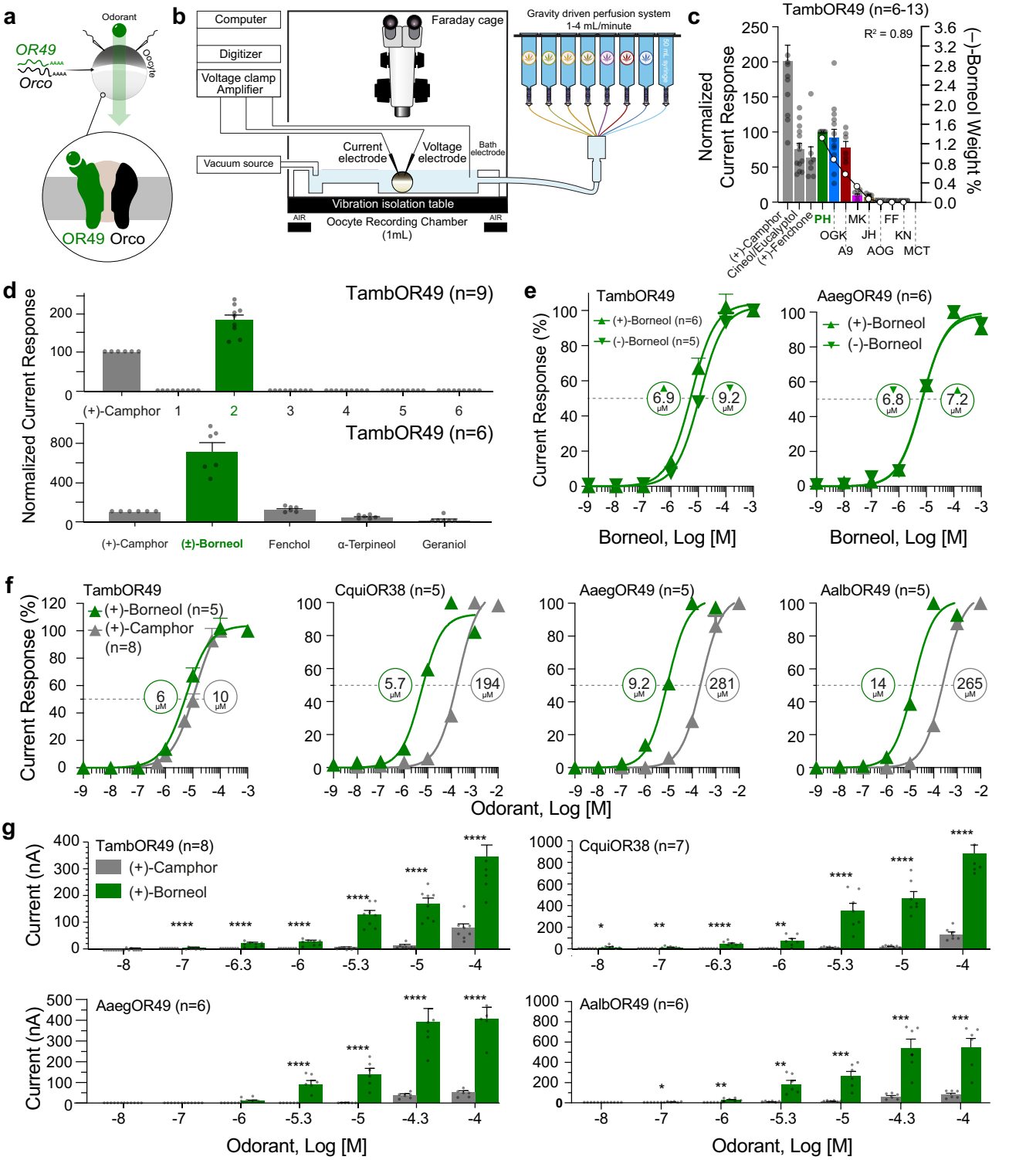

Fig. 2 | Odorant receptor 49 is a selective borneol receptor. a OR49 and Orco mRNA are injected into a *Xenopus laevis* oocyte. Blow up depicts the oocyte's membrane expressing a functional OR49-Orco complex**. b** Schematic illustration of the TEVC set-up. **c** Pineapple Haze (PH), OG Kush (OGK), Adom9 (A9), and Master Kush (MK) elicited the highest currents from TambOR49. Bars correspond to the left Y-axis. Borneol content (solid white circles) is indicated on the right Y-axis. A correlation between the OR49 response and the borneol content in each *Cannabis* EO was observed ($R^2 = 0.89$). (±)-Camphor n = 13, cineol $n = 13$, fenchone $n = 7$, PH $n = 6$, OGK $n = 13$, A9 $n = 6$, MK $n = 6$, JH $n = 6$, AOG $n = 6$, FF $n = 6$, KN $n = 6$ and MCT $n = 6$. **d** Response of TambOR49 to 6 *Cannabis* sub-mixtures and the constituents from sub-mixture 2. **e** Concentration-response relationships of TambOR49 and AaegOR49 to the two borneol enantiomers. **f** Concentration-response relationships of TambOR49, *Culex quinquefasciatus* OR38 (CquiOR38), *Ae. aegypti* OR49 (AaegOR49) and AalbOR49 in response to (+)-borneol and (+)-camphor. Effective concentrations at 50% of the maximal response (EC_{50}) were calculated using Graphpad Prism 8 and are shown and given in µM units. **g**, Pairwise comparisons of the current responses of all four mosquito species OR49s elicited by increasing concentrations of (+)-borneol and (+)-camphor. Statistical differences were evaluated by multiple t-tests. $^*p < 0.05$, $^{**}p < 0.01$, $^{***}p < 0.001$ and $^{****}p < 0.0001$. Data are presented as mean values +/- SEM. Representative current traces can be found in Supplementary Fig. 3. Source data are provided as a Source Data file. 'n' refers to the number of biological replicates.

https://doi.org/10.1038/s41467-026-69511-z

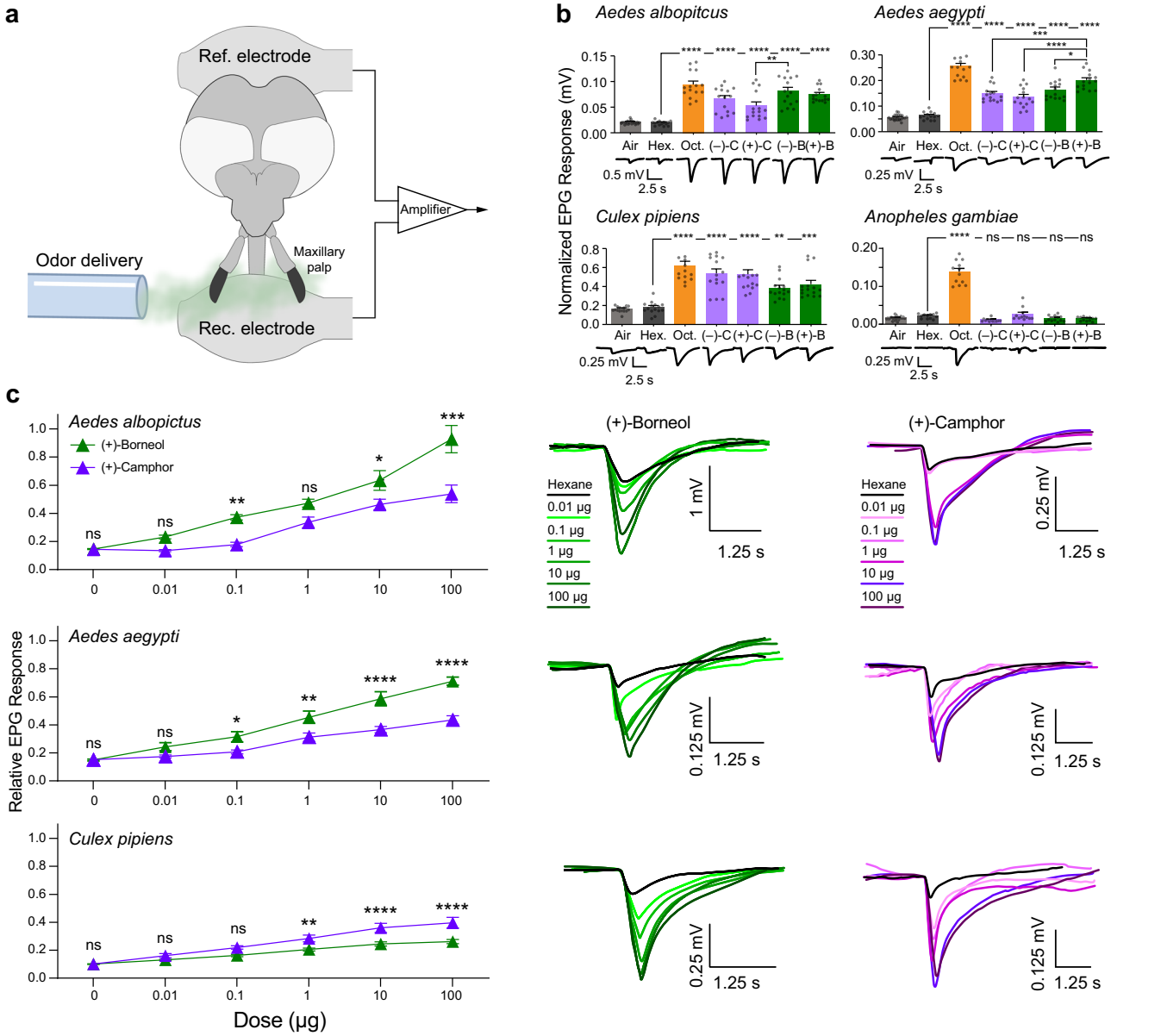

Fig. 3 | The maxillary palp of culicine mosquitoes respond to borneol and camphor. a Schematic illustration of the Electropalpogram (EPG) set-up. **b** EPG responses in *Aedes albopictus*, *Aedes aegypti*, *Culex pipiens*, and *Anopheles gambiae* to 1-octen-3-ol (orange, 10 µg), camphor (purple, 10 µg), and borneol (green, 10 µg) enantiomers relative to hexane. Representative traces for each odorant are shown below the X-axis. Statistical differences were evaluated via one-way anova. $^{*}p < 0.05$, $^{**}p < 0.01$, $^{***}p < 0.005$ and $^{****}p < 0.001$. Data are presented as mean values +/- SEM, $n = 15$. Only significant statistical differences are shown. **c** Dose-response relationships of the maxillary palps of three culicine mosquito species in response to increasing concentrations of (+)-borneol and (+)-camphor. Representative traces are shown on the right. Statistical differences were evaluated via two-way ANOVA. $^{*}p < 0.05$, $^{**}p < 0.01$ and $^{****}p < 0.001$. Data are presented as mean values +/- SEM, $n = 15$. Source data are provided as a Source Data file.

the cpA and cpB neurons to CO_2[22] (data not shown) and *R*-(−)−1-octen-3-ol[23], respectively, has been well characterized in previous studies[13–15]; note that two previous studies have identified cpC as the *R*-(−)−1-octen-3-ol responding neuron in *Ae. aegypti*[14,24], which may be due to differences in genotypes used. (+)-Borneol elicited a dose-dependent response in the cpC neuron of *Ae. aegypti* (Supplementary Fig. 7), *Ae. albopictus*, *Cx. quinquefasciatus* but not in *An. gambiae s.s.* (Fig. 4b). Single sensillum recordings identified the spontaneous activity of three sensory neurons housed in the capitate peg sensilla of wild-type *Ae. aegypti* (Fig. 4c) and *An. gambiae*, which are clearly distinguishable by differences in spike amplitudes (Fig. 4d). No SSR responses were recorded from the cpC neuron in the *Ae. aegypti Or49* null mutant line in response to (+)-borneol (Fig. 4c), indicating that *Or49* is necessary to confer the cpC neuron sensitivity to borneol. Although recordings were not obtained from the cpA and cpB neurons in the *Or49* null mutant, these neurons displayed normal spontaneous activity (Supplementary Fig. 8). We note that the reduced longevity of the mutant line could potentially affect neuronal function; however, no such effect was observed. The lack of response of the cpC neuron in *Anopheles* (Fig. 4d) is consistent with the expression of *Or28* instead of *Or49*, which is not activated by borneol (Supplementary Fig. 5). The absence of OR28 activation and *An. gambiae* palp EPG responses by borneol and camphor supports this conclusion.

Borneol and camphor specifically activate the MD3 glomerulus in the antennal lobe

To examine how *Ae. aegypti* processes borneol in the antennal lobe (AL), two-photon imaging experiments were conducted using pan-

https://doi.org/10.1038/s41467-026-69511-z

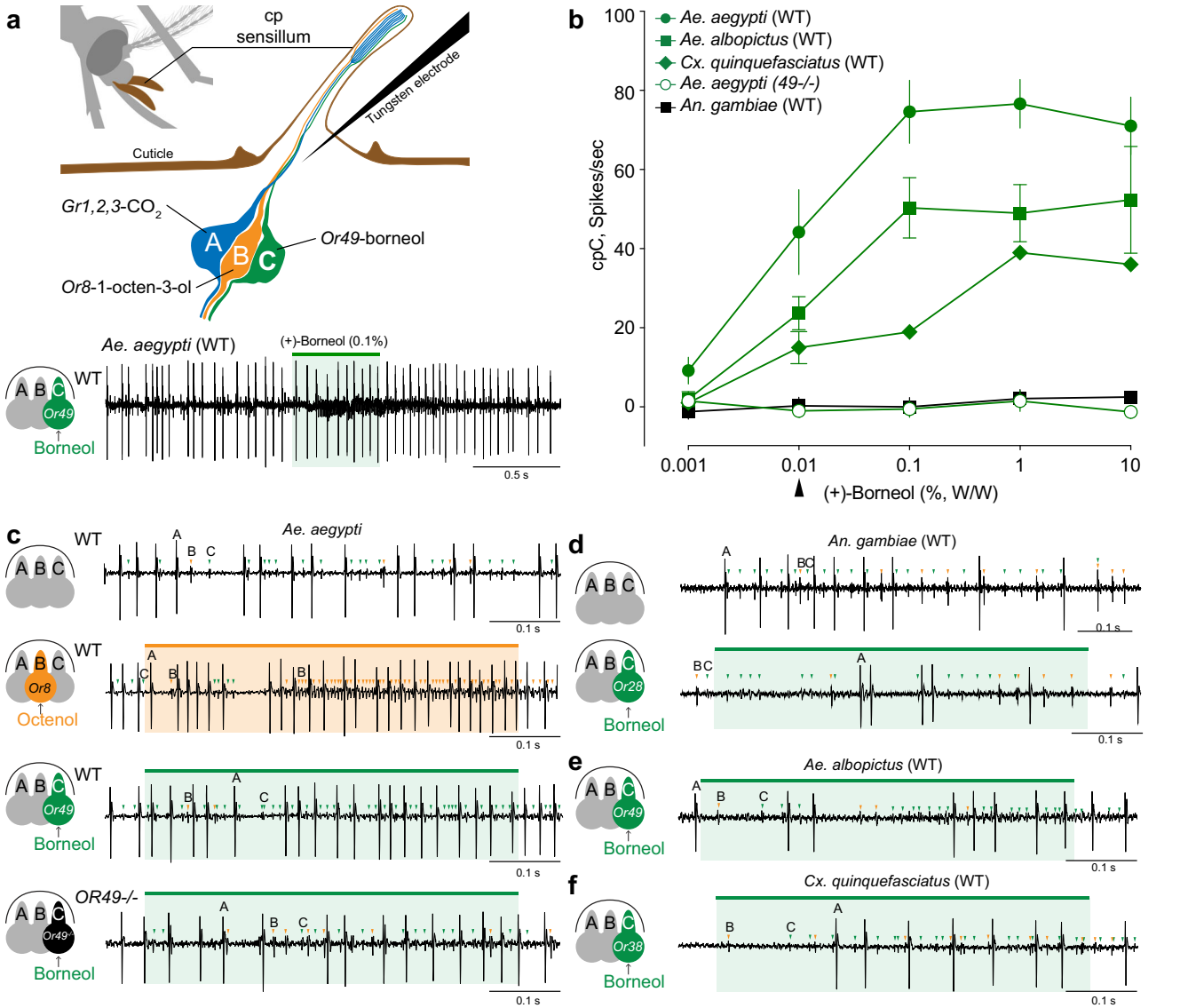

Fig. 4 | Species-dependent response to (+)-borneol of the C neuron of the capitate peg sensilla and its reliance on *Or49* in *Ae. aegypti*. **a** A tungsten electrode was used to record action potentials (spikes) from the capitate peg sensillum on the maxillary palp, which houses three neurons. A representative single sensillum recording (SSR) trace illustrates neuronal activity during the one-minute intervals preceding and following borneol stimulation. At this temporal scale, the cpA neuron is readily identified by its large-amplitude spikes and its known responsiveness to CO_2. The cpB and cpC neurons, while more similar in spike amplitude, can be distinguished at higher temporal resolution. **b** Species- and dose-dependent response of the C neuron to (+)-borneol with mean ± s.e.m. at each concentration. The arrow and dotted line indicate the borneol dose to the shown representative traces. *Ae. aegypti* ($n = 10$), *Ae. albopictus* ($n = 7$), *Cx. quinquefasciatus* ($n = 2$), *Ae. aegypti Or49*$^{-/-}$ ($n = 8$), *An. gambiae* ($n = 15$). Data are presented as mean values +/- SEM. **c** Top trace shows the spontaneous activity of the three sensory neurons in the capitate peg sensilla of WT *Ae. aegypti*. Note the differences in spike amplitude of the A, B (orange markers), and C neurons (green markers). Middle traces show responses to *R*-(−)−1-octen-3-ol and (+)-borneol in the B and C neurons of WT *Ae. aegypti*, respectively. Bottom trace shows how the response to (+)-borneol is abolished in *AaegOr49*$^{-/-}$ mutant mosquitoes. **d** top - The spontaneous activity of the three sensory neurons in the capitate peg sensilla of WT *Anopheles gambiae s.s.* bottom - The C neuron of *An. gambiae s.s.* does not respond to (+)-borneol. **e**, **f** Representative traces of the cp sensilla of *Ae. albopictus* and *Cx. quinquefasciatus*. Source data are provided as a Source Data file.

neuronal GCaMP-expressing Ae. aegypti mosquitoes. We utilized existing mosquito lines that contained a *QUAS-GCaMP7s* transgene crossed with the *brp-QF2* driver line[25], allowing the directed expression of the calcium indicator GCaMP7s in all neurons of the AL. Mosquitoes were glued to holders that permitted two-photon imaging of calcium responses in the AL (Fig. 5a), allowing repeatable registration of the AL glomeruli between preparations (Fig. 5b, S10) and recording of glomerular responses (Fig. 5c)[26]. Glomeruli from our two-photon imaging results were mapped to AL atlases[27,28], allowing accurate identification of the glomeruli of interest in their spatial context (video rendering of the antennal lobe in Supplementary Movie 1). We focused on the mediodorsal (MD) glomeruli, using the most recently published AL atlas[27], as these glomeruli receive input from the capitate peg sensilla of maxillary palps (Fig. 5b, c, S10) and are responsive to host odors, including 1-octen-3-ol (MD2) and CO_2 (MD1)[28].

To determine the odor coding of the mediodorsal glomeruli, and identify the cognate glomerulus representing borneol, we concentrated on recording from the MD3 glomerulus and stimulating with borneol (10^{-4} dilution). Next, we examined responses of the MD1 and 2 glomeruli if they occurred in the same imaging plane while stimulating with CO_2 (5%), 1-octen-3-ol (10^{-4} dilution), borneol (10^{-4} dilution), and the solvent control. For the MD3 glomerulus, (+)-borneol elicited strong, tonic responses that were significantly greater than the solvent control (Kruskal-Wallis test, $P = 0.006$) (Fig. 5d, g). By contrast,

https://doi.org/10.1038/s41467-026-69511-z

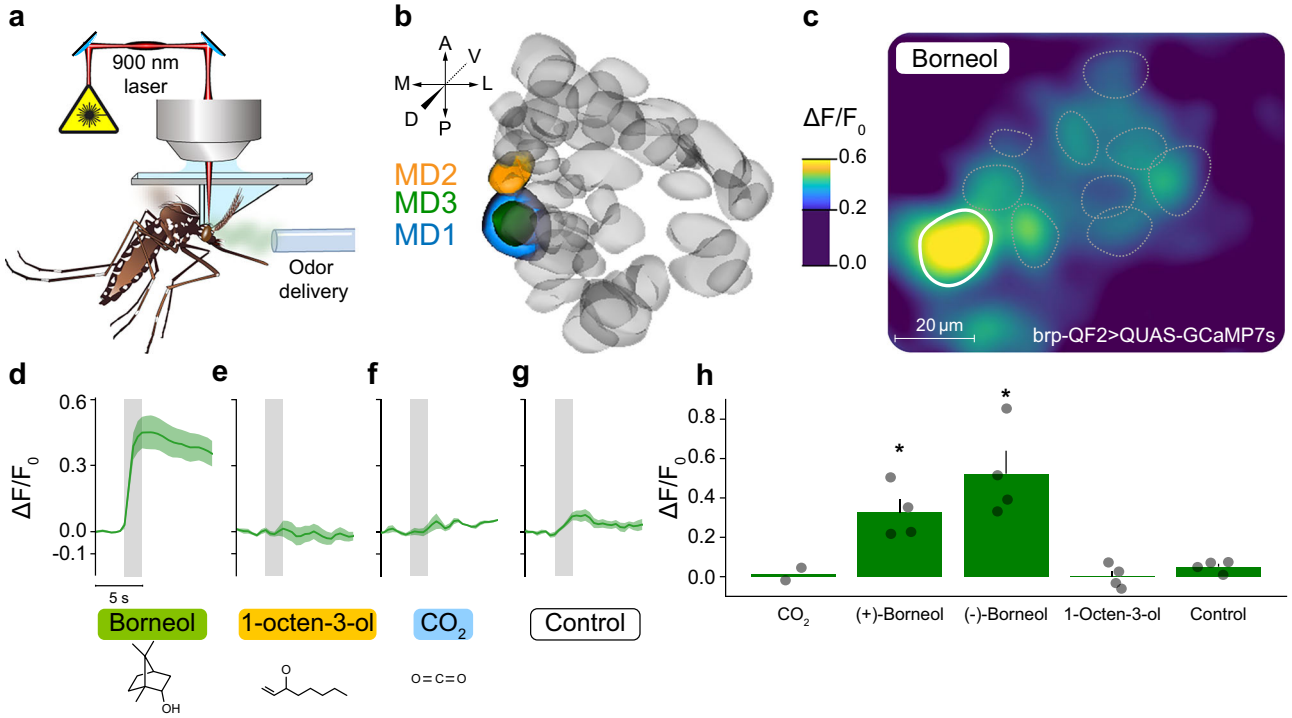

Fig. 5 | Borneol elicits robust responses in the *Ae. aegypti* AL. a Schematic of the two-photon setup used to record calcium dynamics in the mosquito antennal lobe (AL). **b** AL atlas, highlighting the MD1 (blue), MD2 (orange), and MD3 (green) glomeruli. Non-responsive AL glomeruli (grey) and the mediodorsal glomeruli were registered and mapped to previously published atlases. **c** Pseudo color plot from a single preparation of $\Delta F/F_0$ calcium responses (0-0.6 scale) to (+)-borneol (10^{-4} dilution), at a depth of 75 µm from the surface of the AL. Borneol evoked a strong response in the region of interest mapped to the MD3 glomerulus (highlighted in white). **d** MD3 glomerulus responses ($\Delta F/F_0$) to (+/-)-borneol and other olfactory stimuli (**e**–**g**). Lines and shaded areas represent mean +/- SEM across mosquitoes. For each odor and animal, repeated stimulations (including both (+)- and (−)-borneol where available) were averaged to obtain a mean response. Data are from 4 of 6 original preparations - mosquitoes 1 and 4 were excluded due to excessive 3D movement of the sample and inconsistent imaging plane caused by sample rotation, respectively. Resulting sample sizes are $n = 4$ mosquitoes for (+/−)-borneol, 1-octen-3-ol (10^{-4} dilution) and solvent control, and n = 2 mosquitoes for CO_2 (5%). The grey bar denotes stimulus duration (2 s). All panels were analyzed as in (**d**). **h** Responses of the MD3 glomerulus to a limited panel of three odorants at 10^{-4} concentration (n = 4), CO_2 (5%) (n = 2), and the negative control (n = 4). Asterisks denote stimuli significantly greater than control (Kruskal-Wallis with multiple comparisons: $p < 0.02$). Responses to CO_2 are not considered in this analysis due to the small sample size. Data are presented as mean +/- SEM. Source data are provided as a Source Data file.

responses of the MD1 and MD2 glomeruli to borneol were not significantly different from the control (P = 0.18 and 0.31, respectively). Similarly, the MD2 glomerulus showed the strongest response to 1-octen-3-ol and the MD1 glomerulus to CO_2 (Supplementary Fig. 9). There was no significant difference between borneol enantiomers (Kruskal Wallis test with multiple comparisons, $P > 0.93$), although borneol evoked significantly greater responses than the solvent (hexane) control (Kruskal Wallis test with multiple comparisons, $p < 0.05$) (Fig. 5g, S9). These findings are consistent with previous studies demonstrating that the three MD glomeruli receive input from the maxillary palp cp neurons, whereby the MD1 glomerulus receives CO_2 input from the cpA neurons[29] while the medium-sized MD2 glomerulus (previously labeled as MD3[28]) receives 1-octen-3-ol input from the cpB neurons[28].

Borneol repellency in human-host-seeking female *Ae. aegypti* is largely mediated by *Or49*

As the mutant lines initially used for SSR exhibited reduced behavioral activity, we generated a new homozygous *Or49* knockout line after backcrossing for six generations and focused on behavioral validation to assess borneol's repellency. To examine whether (+)-borneol's repellency to blood-seeking *Ae. aegypti* mosquitoes is mediated by *Or49*, we conducted an arm-in-a-cage assay. Fifteen WT and *Or49* K.O. females were exposed to human skin odor in the presence and absence of (+)-borneol, for 10 minutes (Fig. 6a). A protective glove covered the hand, allowing mosquitoes to detect the odor through a dorsal open area, which was protected with a screen and equipped with a chemical holder for the deposition of (+)-borneol (1 M) (Fig. 6a, Supplementary Fig. 10). Although the setup allows for potential contact between mosquitoes and the borneol-soaked filter paper, we did not observe any instances of direct physical interaction.

Our results show that under (+)-borneol exposure, wild-type females exhibited an average reduction of 54% in visits to the ROI compared to the vehicle control, whereas *Or49*$^{-/-}$ mutants displayed a more modest reduction of 25% compared to their respective vehicle control (Fig. 6b). Representative behavioral traces and detections are shown in Fig. 6e and Supplementary video 2. The repellent effect of (+)-borneol in WT mosquitoes was observed mainly at the first three minutes of the experiment. Contrary to this, *Or49* null mutants behaved similarly to the control conditions (i.e., without (+)-borneol) (Fig. 6c). To assess the mixed effects of visit rates, time intervals, and their interaction, we performed a Generalized Linear Mixed Model (GLMM) with biological replicates included as a random effect. Under control conditions (Hand + diethyl ether), there was no significant difference in the number of visits to the region of interest (ROI) between genotypes (p = 0.492), and no significant interaction between genotype and time ($p = 0.309$). However, both WT and KO mosquitoes exhibited a significant reduction in visit rates over time ($p < 0.001$), consistent with a gradual decline in exploratory activity (Fig. 6d top Supplementary Data 2). In the presence of (+)-borneol, visit rates diverged significantly between strains. WT mosquitoes displayed consistently low visit rates, while KO mosquitoes made significantly

https://doi.org/10.1038/s41467-026-69511-z

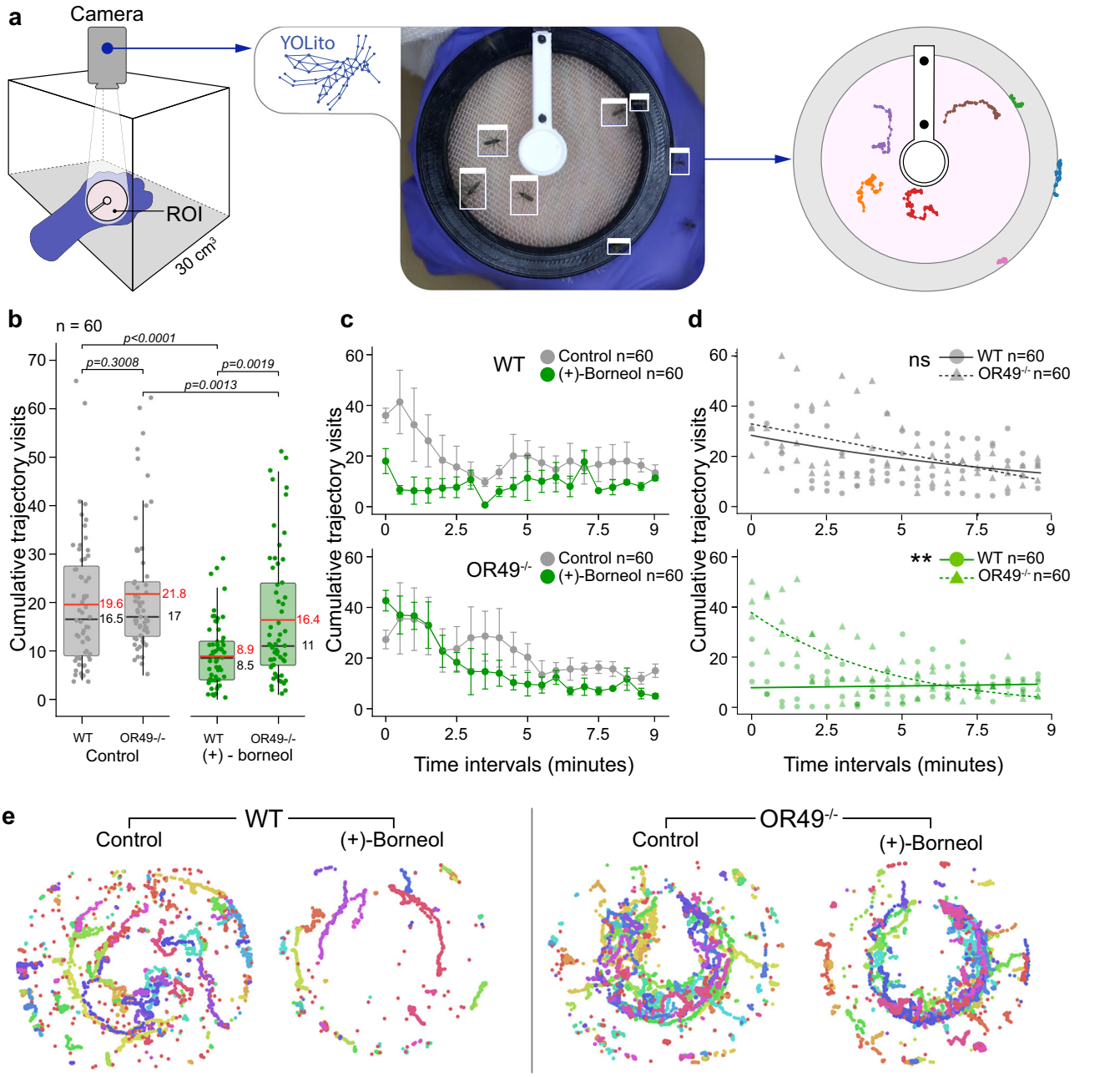

Fig. 6 | Borneol repellency is mediated largely by *Or49* in host-seeking female *Ae. aegypti* (Liverpool). a Schematic of the behavioral assay, representative image showing model predictions, and illustration of mosquito trajectory tracing. **b** Boxplots showing the cumulative number of visits by wild-type (WT) and odorant receptor 49 knockout ($Or49^{-/-}$) female mosquitoes within the region of interest (ROI) under control (Human odor + DEE) and treatment (Human odor + DEE + (+)-borneol). Gray data points indicate exposure to control conditions, whereas green data points indicate exposure to treatment conditions. Each data point represents the cumulative number of visits within a 30 sec interval (applies also to **c** and **d**). Boxplots show the interquartile range (25th–75th percentiles), with medians (black line) and means (red line); whiskers extend to ± 1.5 x IQR, and outliers are shown as individual points. Pairwise comparisons were assessed using two-sided Mann–Whitney U tests; exact *p* values are shown, and U statistics are reported in Supplementary Data 4. **c** Time course of cumulative mosquito visits. Data points represent the mean ± SEM of three biological replicates at each time point. **d** Generalized linear mixed model (GLMM) predictions for visit counts. The model was fitted using a Poisson error distribution with a log link function. Treatment, time interval, and their interaction were included as fixed effects, with biological replicates included as a random intercept. Statistical inference was based on two-sided Wald *z* tests with asymptotic degrees of freedom. Lines indicate model-predicted values, and points represent the cumulative number of visits per treatment and biological replicate at each time point. A significant treatment effect was observed in the (+)-borneol condition (estimate = 1.59 ± 0.27 SE, $z = 5.81$, $p = 6.26 \times 10^{-9}$), along with a significant treatment × time interaction (estimate = −0.24 ± 0.02 SE, $z = -12.44$, $p < 2 \times 10^{-16}$), indicating a differential temporal response. No significant treatment effect or interaction was detected in the control comparison (treatment: estimate = 0.15 ± 0.28 SE, $z = 0.54$, $p = 0.587$; interaction: estimate = −0.022 ± 0.014 SE, $z = -1.53$, $p = 0.127$; Supplementary Data 5). **e**, Representative mosquito trajectories under each treatment condition. Source data are provided as a Source Data file.

more visits (strain effect: $p < 0.0001$), with a significant strain × time interaction ($p < 0.0001$), indicating differential behavioral trajectories over the course of the assay (Fig. 6d, bottom; Supplementary Data 2). Wild type mosquitoes showed no significant change in the number of visits over time ($p = 0.668$), indicating a stable avoidance response. In secondary behavioral metrics, WT and $Or49^{-/-}$ mosquitoes showed no significant difference in walking distance ($p = 0.09$) or visit duration ($p = 0.55$) when exposed to the hand alone (Data S4). In contrast, $Or49^{-/-}$

mosquitoes exhibited a significant increase in visit duration ($p = 0.005$) under borneol exposure (Supplementary Fig. 11; Supplementary Data 2). Full trajectory data for all treatments are provided in Supplementary Fig. 12.

Discussion

We have identified a conserved mechanism in culicine mosquitoes responsible for the selective detection of borneol, a bicyclic monoterpenoid that has been used as an insect repellent since ancient times. Recent studies have shown that borneol is a broad-acting insect repellent against fungus gnats[30], the booklouse *Liposcelis bostrychophila*[31] and fire ants[32]. These findings suggest that multiple olfactory-mediated mechanisms operate in insects, as *Or49* homologs have not been identified in these species. Interestingly, borneol elicits responses in the *Ae. aegypti* antenna as well[33]. However, this alternative mechanism is *Or49*-independent since its expression has not been reported in the antenna. We have surveyed the activation of glomeruli in ROI adjacent to the MD region and did not detect any other borneol-activated glomeruli (Supplementary Fig. 9).

In *Anopheles*, the antennal-expressed *Or48*[34], one of the two closest homologs to the culicine *Or49* (Supplementary Fig. 1c), responds to straight chains alcohols, ketones, and acetates[18,35] suggesting that this receptor is tuned to a different class of compounds, setting apart the olfactory coding logic between these two mosquito subfamilies. Contrary to OR8, which discriminates between the 1-octen-3-ol enantiomers[21], the two borneol enantiomers elicited comparable activations at the pharmacological, physiological, and AL levels. These findings suggest that the receptor binding pocket accommodates both forms of borneol or that a closely related structural analog of borneol, with greater potency, remains to be identified [36].

Our results suggest that in *Ae. aegypti* and other culicine mosquitoes, the repellent properties of traditional Chinese medicinal plants such as the camphor tree EO are mediated in part by the activation of OR49 by bicyclic monoterpenoids and more specifically by borneol. Borneol repels human host-seeking *Ae. aegypti*, *Cx. quinquefasciatus* and *An. stephensi*[33,37,38] while its presence in EOs attracts gravid *Ae. aegypti*[39], suggesting that this compound has opposite effects on animal-host-seeking behavior and oviposition preferences. The reason for borneol being a signal mediating repellency is puzzling. While several monoterpenoids such as 1,8-cineole, limonene, and fenchone exhibit anticholinesterase activity[40,41] causing paralysis and death in a variety of insects, there are conflicting reports on the larvicidal activity of borneol and camphor against mosquito larvae[39,42–45]. Future studies should focus on the ecological role of borneol in different contexts, including foraging and oviposition site selection.

Our findings indicate that the cp sensillum in the palp of culicine mosquitoes detects signals from animal and plant hosts. Why OR49 shows such strong selectivity for borneol, among the many plant-derived volatiles known to repel mosquitoes, remains an open question. Further experiments will reveal how these three signals are integrated at the pre-synaptic level within the sensillum and in the AL. Understanding the ecological and neurological significance of the mosquito cp sensillum, i.e., the packaging of animal and plant host detectors within the same sensillum, may be exploited to design novel repellent formulations.

Our behavioral assay demonstrated that OR49 is required for a full behavioral avoidance response to (+)-borneol. WT mosquitoes exhibited immediate and sustained suppression of ROI visits under repellent exposure, consistent with effective stimulus detection and aversive action. The absence of a time-dependent decline in the WT group further supports the idea that repellency is exerted early and robustly. By contrast, $Or49^{-/-}$ mutants exhibited a higher number of visits and a behavioral pattern that closely resembled control conditions, suggesting a reduced ability to detect or respond to (+)-borneol. Although avoidance was not abolished in the KO strain, the attenuated response indicates that *Or49* contributes to (+)-borneol detection, while alternative receptors or pathways provide a comparable contribution through overlapping sensitivity to borneol and related terpenoids. The lack of change in walking distance and visit duration in WT mosquitoes likely reflects their limited engagement with the ROI due to early avoidance, whereas the increase in both metrics in KO mosquitoes suggests that, in the absence of effective detection, these individuals continued to explore the ROI. This pattern implies a partial or delayed response, possibly mediated by additional receptors with lower sensitivity to borneol. Together, these findings establish OR49 as a central, though not exclusive, mediator of (+)-borneol-induced avoidance and provide behavioral evidence linking olfactory receptor function to time-stable repellency.

Our data provide functional evidence that the 3 MD glomeruli receive afferent fibers from the maxillary palp[46]. Whether the grouping of these three glomeruli has a functional significance and why the cp sensillum houses ORNs tuned to animal and plant host olfactory cues should be the focus of future studies. The two largest cp neurons are tuned to animal-host attractants, whereas the smallest and third cpC neuron responds to a plant-host odorant with repellent activity. This antagonism in valence, whereby an attractive signal is detected by the largest of two ORNs within the same sensillum while a deterring signal is detected by the smallest ORN, is widespread in animals [47]. We surmise that the main function of the mosquito cp sensillum is to detect animal host odorants, while the cpC neuron exerts a presynaptic inhibitory effect mediated by lateral coupling when activated by borneol.

Methods

Insects

Our mosquito colonies were reared according to previously published protocols[48]. *Ae. aegypti* originated from a colony established by Prof. Joel Margalit. The *Ae. aegypti* Liverpool strain was provided by the Akbari lab. *Aedes albopictus* was the FPA Foshan strain collected (Foshan, China) reared at the insectary of the University of Pavia since 2013 (Palatini et al., 2017). *Anopheles gambiae* was the G3 strain originally isolated from West Africa (MacCarthy Island, The Gambia) in 1975 (Federica Bernardini et al., 2017). *Culex pipiens* originated from a wild type population that was provided by Dr. Laor Orshan (Ministry of Health, Israel).

Phylogenetic and genomic analyses

The AaegOR49 protein sequence (AAEL001303-PA) was used as a query to identify homologs in other mosquito species. Amino acid sequences of homologous ORs were obtained from the Vectorbase database (vectorbase.org) and the *Tx. amboinensis* genome assembly[49]. The multiple sequence alignment was conducted using ClustalW[50]. The Maximum-likelihood phylogenetic tree was constructed using MEGAX software (Model: G, bootstraps: 5000). Exon-intron structure analysis was conducted manually by aligning predicted amino-acid sequences to genomic regions. Approximate mapping of the genes in chromosome location for each mosquito species and construction of synteny maps were done using Geneious Prime software[51] using the latest genome assemblies available for each mosquito species[20,52–55].

Genomic DNA (gDNA) was isolated from whole bodies of *Tx. amboinensis* adults. gDNA was diluted to 25 ng/μL in nuclease free water and used as a template in polymerase chain reactions to amplify odorant receptors (TambOR) using Taq polymerase and the following primer sets: TambOr6.F1 (ATGCGCTTCTACGAGAAATAC), TambOr6.R1 (TCAGAAATTATCCTTCAGGATC); TambOr12.F1 (ATGCCATCGGTTTTCTTGGTT), TambOr12.R1 (CTAAAACACTCGCTTCAATATC); TambOr13.F1 (ATGTTCTGCTTCAGGAAGATC), TambOr13.R1 (CTAGAAGTGGTTTTTCAATATAA); TambOr49.F1 (ATGTTGTTCAAGAACTGTTTCC), TambOr49.R1 (TTAATAATTGAATCTTTCCTTCAG);

TambOr71.F1 (ATGGGCAGCAGTGATGGTGAC), TambOr71.R1 (CTACT GGTTGATTTTACTGAGG). Cycling conditions were 94 °C for 60 s; 30 cycles of 94 °C for 20 s, 56 °C for 20 s, 72 °C for 30 s; and a final extension of 72 °C for 5 minutes. Amplicons were analyzed by electrophoresis on a 1% agarose gel, cloned into the TOPO-TA pCR2 plasmid, heat-shock transformed into TOP10 competent *E. coli* cells, and grown overnight at 37 °C on LB+ampicillin+X-gal agar plates. Ampicillin-resistant, white colonies were isolated using a sterile pipette tip and grown overnight at 37 °C in 3 mL of LB+ampicillin. Plasmids were isolated by DNA miniprep, and the Sanger method was used to determine the DNA sequence in both directions using standard T7 and M13.rev primers. TambOR nucleotide sequences were compiled into contigs and intron/exon regions were inferred by comparing to coding sequences described in a previous publication[49].

Chemical reagents

The chemicals used for the deorphanization of receptors were obtained from Acros Organics (Morris, NJ, USA), Alfa Aesar (Ward Hill, MA, USA), ChemSpace (Monmouth Junction, NJ, USA), Sigma Aldrich (St. Louis, MO, USA), TCI America (Portland, OR, USA), Thermo Fisher Scientific (Waltham, MA, USA), and Penta Manufacturing Corp. (Livingston, NJ, USA) at the highest purity available. *Cannabis* EOs and sub-mixtures were formulated and supplied by Eybna Technologies (Kfar Saba, Israel) (Supplementary Data 1 and Supplementary Fig. 2,4).

Two-electrode voltage clamp of *Xenopus laevis* oocytes

In vitro transcription and two-microelectrode voltage clamp electrophysiological recordings were carried out as previously described[56]. Experimental procedures for the *Ae. albopictus* receptor clone was performed as previously described[57]. *AalbOr49* and *AalbOrco* templates were synthesized by Twist Biosciences (San Francisco, CA, USA) and cloned into the pENTR^{TM} vector using the Gateway^{R} directional cloning system (Invitrogen Corp., Carlsbad, CA, USA) and subcloned into the *X. laevis* expression destination vector pSP64t-RFA. Several of these genes were codon-optimized (Supplementary data 2). The EC_{50} values were calculated using Graphpad Prism 8. Briefly, after data collection, the data of each oocyte was normalized against its highest response. This was done to overcome the high variance between individual oocytes. After normalization, the data of each oocyte was analyzed using the function "Nonlinear regression" with "Dose – response – Stimulation" equation "log(agonist) vs. normalized response". This function yields the EC_{50} value for each repetition (at least five oocytes). The EC_{50} values were then analyzed for the average and S.E.M values (Supplementary Fig. 13). For pairwise current comparisons of (+)-borneol and (+)-camphor, two separate perfusion systems were assembled, one for each compound. The outlet from each system was connected to a 2 to 1 perfusion manifold. At each tested concentration, (+)-borneol and (+)-camphor were administered consecutively. Representative current traces can be seen in Supplementary Figs. 3 and 5. *Odorant receptor 49* and *Orco* clones and recording measurements can be found in Supplementary Data 2 and 3, respectively. The use of *Xenopus laevis* frog eggs was carried out according to The Hebrew University of Jerusalem Ethics committee (NIH approval number: OPRR-A01-5011). The list of *Or* nucleotide sequences for injection in *Xenopus* oocytes can be accessed in Supplementary data 2.

Electropalpogram recordings

Based on the voltage clamp data, responses from the maxillary palps of *Ae. albopictus*, *Ae. aegypti*, *Cx. pipiens* and *An. gambiae* were recorded with camphor or borneol. Electopalpogram (EPG) assays were performed according to published procedures[58] with a few modifications. Within the Pasteur pipette, 20 µL of odorants diluted in hexane were deposited at the desired dose onto a 4 × 20 mm Whatman filter paper strip. The odorants were delivered into a consistent humidified airstream (at a flow rate of 50 cm/s) at approximately 2 cm from the maxillary palps. The pulse duration was 0.1 s, and the recording time was set for 5 s. A 2-min gap was allowed between stimuli to recover the EPG sensitivity. At least 5 individual females were tested, for each individual, 3 technical replicates were performed with doses ranging from 0.01 ug to 100 µg. Negative controls (hexane and air) and positive controls (1-octen-3-ol) were performed at both the beginning and end of each recording session to monitor the decline in sensitivity of the maxillary palps. EPG peak responses were normalized to the response of hexane.

Generating *Or49* knockout line in *Ae. aegypti* and isolating an *Or49*$^{-/-}$ homozygous line

Genomic DNA was extracted from whole bodies of *Ae. aegypti* Liverpool individuals using the DNeasy Blood & Tissue Kit (Qiagen, Redwood City, CA). Homology arms of the *Or49* gene flanking 1 kb upstream and downstream of the desired insertion site (Supplementary Fig. 6a) were amplified with the Q5 High Fidelity DNA polymerase (New England Biolabs, Ipswich, MA), using primer pairs Left_Arm_Or49_FWD and Left_Arm_Or49_REV as well as Right_Arm_Or49_FWD and Right_Arm_Or49_REV, respectively (Supplementary Data 3). The QF2-ECFP DNA cassette was amplified using the V1117A plasmid as template and the primer pair QF2_OpIE_ECFP FWD and QF2_OpIE_ECFP REV. PCR bands were cut out from agarose gels and purified with Zymoclean Gel DNA Recovery Kit (Zymo Research, Irvine, CA). Upstream and downstream homology arms, as well as the QF2-ECFP cassette PCR products, were assembled into the backbone of the V1117A plasmid using Gibson assembly reaction, following the manufacturer's recommendations. Gibson's reaction-derived plasmid product was used to transform JM109 cells (Zymo Research), and colonies were individually grown overnight for minipreps with Zyppy Plasmid Miniprep Kit (Zymo Research). The sequence of the plasmid V1117F-Or49 (Supplementary Fig. 6b) was confirmed by restriction enzyme digestion using the enzymes ScaI-HF and AvrII as well as by whole plasmid sequencing (Primordium Labs, Monrovia, CA). V1117F-Or49 plasmid was used to retransform JM109 cells, which were grown for maxiprep purification using the PureLink Expi Endotoxin-Free Maxi Plasmid Purification Kit (Thermo Fisher Scientifics, Waltham, MA).

For guide RNA synthesis, non-template reactions were carried out with the gRNA_Left_Or49_F and gRNA_Left_Or49_R forward primers and the universal guide RNA reverse primer (Universal-sgRNA_R). PCR bands were isolated from agarose gel and purified as described above (Supplementary Fig. 6c). Guide RNAs were synthesized with the Ambion MEGAscript kit (Thermo Fisher Scientifics) for 4 hours at 37 °C, using 300 ng of purified PCR product. Guide RNAs were further purified with the Megaclear Kit (Thermo Fisher Scientifics).

To assess the cleavage activity of the synthesized guide RNAs, in vitro Cas9 cleavage assays were carried out. A DNA fragment spanning 1,009 bp overlapping the cleavage sites of the guide RNAs was amplified with primers Or49_cleav_F and Or49_cleav_R, DNA bands were isolated from agarose gel, purified, and 100 ng of which was used in cleavage assays with 300 ng of recombinant Cas9 (PNA BIO, Thousand Oaks, CA) and 100 ng of each guide RNA upon incubation at 37 °C for 1 hour.

For embryo microinjection, an injection mix was prepared with the plasmid V1117F-Or49 at 500 ng/ul, gRNAs left and right at 100 ng/ul each, and recombinant Cas9 at 300 ng/ul. Mix was filtered with the Ultrafree-MC Centrifugal Filter UFC30GUOS (Millipore, Burlington, MA). Freshly harvested *Ae. aegypti* embryos (Liverpool strain) were injected with the transformation mix using a custom-made insect embryo microinjector (Hive Technologies, Cary, NC) at 100 psi pulse and 3 psi back pressures, using quartz needles pulled with a P-2000 needle puller (Sutter Instrument Co., Novato, CA). Genomic DNA of the G1 fluorescent mosquitoes (Supplementary Fig. 6d) was individually extracted with the Qiagen blood kit. For whole DNA cassette sequencing (Primordium), 2.5 kb DNA fragments were amplified from the DNA

of G1 individuals using the primer pair Or49_diag_up_F and Or49_diag_down_R (Supplementary Fig. 6e).

For isolation of homozygous knockout individuals, pupae were sex sorted, and single pairs were transferred into Narrow *Drosophila* Vials (Genesee Scientific, El Cajon, CA), filled with 10 mL of deionized water (DI) and closed with cotton stoppers. Upon emergence, water was drained, and sugar cottons were placed into the vials. Mosquitoes were allowed to mate for 5 days in the vials, and then all individuals were transferred to a single cage for blood feeding. Three days after blood feeding, females were individually transferred to a fresh vial containing a piece of brown paper towel wetted with 1 mL DI water. Females were allowed to lay eggs, and each egg batch was individually hatched in 250 mL Clear Pet Cups (9 oz). Larvae were screened for fluorescence, and the batches that resulted in 100% fluorescent individuals were grown to adulthood and intercrossed to confirm homozygosity in the following generation. Two out of thirty egg batches resulted in homozygous offspring. To further confirm the homozygous status of these individuals, genomic DNA of three pools of 10 males, 10 females, and a mix of males and females were PCR amplified with the primer pair Or49_diag_up_F and Or49_diag_down_R, which resulted in a single band for homozygous individuals and two bands for heterozygous individuals (Supplementary Fig. 6f). To solve the low initial performance of this mutant line in behavioral assays, this line underwent 6 generations of backcross to the wild type line, intercrossed for 3 generations, and a homozygous line was selected as described.

Three primer pairs (Or49_diag_offsite_F/R, *Or49*_amp_F/R, and *Or49*_M13_F/R) that target different regions of the plasmid backbone (Supplementary Fig. 6a) were used to verify whether the plasmid was incorporated into the genome of the *Or49* knockout line (Supplementary Fig. 6g). The *Or49*_diag_up_2F and Or49_diag_down_2R primer pair, which base-pair with genomic sequences outside of the homology arms, on the other hand, were used to amplify the homology arms along with the DNA cassette, in order to amplify the endogenous *Or49* gene (Supplementary Fig. 6h), rather than the sequence of the *Or49* gene of the plasmid that was inserted into the genome.

Single-sensillum electrophysiology

Single sensillum recordings from capitate peg sensilla on the maxillary palp of wild-type female *Ae. aegypti* (Liverpool), *Ae. albopictus* (FPA), *Cx. quinquefasciatus* (Thai) and *An. gambiae sensu stricto* (G3) and *Ae. aegypti Or49*$^{-/-}$ mutant mosquitoes were performed using an established protocol[59]. Spikes were quantified offline using the established nomenclature for the sensory neurons[60]. The number of spikes counted during a 0.5 s stimulus delivery interval was subtracted from the number of spikes counted during a 0.5 s prestimulus period, and the result was multiplied by 2 to obtain the activity of individual sensory neurons housed in the capitate peg sensillum as a spikes/s measurement.

Discrimination between the cpB and cpC neurons is based on spike amplitude, spontaneous activity and their respective functional responses. In our study, the cpB neuron, which is sensitive to 1-octen-3-ol, consistently exhibited larger action potential amplitudes than the cpC neuron, which is activated by borneol. This is in line with several other studies in *Aedes*, *Culex*, and *Anopheles* species that have reported that the cpB neuron is responsive to octenol[13,23,59,61–63]. While other investigations in *Aedes aegypti* have identified the cpC neuron, characterized by the smallest spike amplitude, as the octenol-sensitive neuron these results are ambiguous. The reason for this discrepancy remains unclear, but likely stem from either a misidentification of the sensory neurons[14] or differences in experimental methods or strain variation[24,64].

To investigate the physiological activity of the A, B and C neurons housed in single capitate peg sensilla, CO_2, *R*-(−)−1-octen-3-ol and (+)-borneol were used: gas cylinders containing metered amounts of CO_2 (300, 600, 1200, 2400, or 4800 ppm) and oxygen (20%), balanced by nitrogen (Strandmöllen AB, Ljungby, Sweden) were used to assess the activity of the A neuron; serial decadic dilutions of *R*-(-)−1-octen-3-ol (CAS: 3687-48-7, Penta Manufacturing, Livingston, USA), diluted in paraffin oil, were used to assess the activity of the B neuron; and serial decadic dilutions of (+)-borneol (CAS: 464-43-7, Sigma-Aldrich, St. Louis, MO, USA), diluted in diethyl ether (SupraSolv, Billerica, MA, USA) were used to assess the activity of the C neuron. Stimulation with gaseous CO_2 was by filling Pasteur pipettes with metered amounts of CO_2 (150, 300, 600, 1200, 2400, 4800 ppm) and oxygen (20%), balanced by nitrogen (Strandmöllen AB, Ljungby, Sweden) similar to previously described methodology[65]. After filling, both ends of the pipettes were sealed with Parafilm. For delivery, the Parafilm was removed, and the pipette was immediately connected to the odor delivery system, allowing CO_2 to be administered in the same manner as other odor stimuli. Pasteur pipettes were refilled with CO_2 after each puff to ensure consistent stimulus delivery. A 15 µL aliquot of each dilution of *R*-(−)−1-octen-3-ol and (+)-borneol was pipetted onto a filter paper (5 mm × 15 mm) inserted inside a Pasteur pipette, and the diethyl ether was allowed 15 min to evaporate, before being used for stimulus delivery. All stimuli were delivered into the airstream passing over the maxillary palp preparation.

Calcium imaging in the *Ae. aegypti* antennal lobe (AL)

Odor-evoked responses in the *Ae. aegypti* antennal lobe (AL) were imaged using the brp-QF2 > QUAS-GCaMP7s progeny from the brp-QF2 and QUAS-GCaMP7s parental lines[25]. A total of six 6–8-day-old female mosquitoes were used for all calcium experiments. Each mosquito was cooled on ice and transferred to a Peltier-cooled holder that allowed the mosquito head to be fixed to a custom stage using ultraviolet glue. The stage permits the superfusion of saline to the head capsule and space for wing and proboscis movement[26,66]. Once the mosquito was fixed to the stage, a window in its head was cut to expose the brain, and the brain was continuously superfused with physiological saline[67]. Calcium-evoked responses in the AL were imaged using the Prairie Ultima IV two-photon excitation microscope (Prairie Technologies) and Ti-Sapphire laser (Chameleon Ultra; Coherent; at 1910 mW power). Experiments were performed at 75 µm depth from the dorsal surface of the AL, allowing characterization of the mediodorsal glomerular responses to olfactory stimuli and allowing these glomeruli to be repeatedly imaged across preparations. Scanning other AL regions[26] did not show discernible responses to borneol, although future work will need to thoroughly characterize the glomerular tuning throughout the AL. To record odor-evoked responses in the mediodorsal glomeruli, images were collected from a 110 µm × 83 µm plane every 513 ms (line period of 1 ms), and for each odor stimulus, images were acquired for 25 s, starting 10 s before the stimulus onset. Image data were imported into Matlab (v2017; Mathworks, Natick, Massachusetts) for Gaussian filtering (2 × 2 pixel; σ = 1.5–3) and alignment using a single frame as the reference at a given imaging depth and subsequently registered to every frame to within ¼ pixel. The one-frame offset between odor onset and image acquisition was aligned during post-processing. Odor stimuli were diluted to 10^{-3} and 10^{-4} ethanol (>100%; Sigma), with ethanol used as the solvent control. During an experiment, odor stimuli were separated by intervals of 120 s to avoid receptor adaptation, and odor syringes were used once per preparation to prevent decreased concentration within the cartridge. Calcium responses are calculated as the change in fluorescence and time-stamped and synced with the stimulus pulses. After an experiment, the AL was sequentially scanned at 0.5 µm depths from the ventral to the dorsal surface to provide glomerular assignment and registration between preparations. Glomeruli (down-sampled to 1 μm^3 voxel) were mapped and registered based on the positions and odor-evoked responses of the putative AL3, MD1-3, and AM2 glomeruli, using the most recent

AL atlases[27,28] and the Amira software (v. 6.5, FEI Houston Inc.). Our prior identification of the 1-octen-3-ol sensitive glomerulus used a different atlas [47], which caused us to tentatively identify the glomerulus as MD3[28]. However, here in this study, for each preparation, we outlined and mapped the glomeruli in Amira (v. 6.5, FEI Houston Inc.), and subsequently compared the glomerulus positions to the new atlas[27], allowing us to identify the borneol-sensitive glomerulus as MD3, and the 1-octen-3-ol glomerulus as MD2. Data collected from preparations 1 and 4 were excluded from the analysis due to strong 3D movement and inconsistent imaging plane in those samples.

Behavioral assay

The role of borneol in human host-seeking female mosquitoes was examined with an arm-in-a-cage assay (Fig. 6a) described previously [48] with minor modifications in an air-conditioned room (26 ± 2 °C, 60 ± 5 % RH). Briefly, the experimenter's hand was presented to fifteen 5–10 days post emergence adult females. A three-dimensional-printed interlocking ring with a diameter of 55 mm was used in this experiment (Supplementary Fig S13). The ring was placed over the dorsal side of a nitrile glove (powder-free latex). To evoke human odor and prevent mosquito bites, we replaced the nitrile glove between the two ring components with a plastic net. The interlocking ring included a central odorant delivery platform comprising a 10-mm-diameter cover glass and two 5-mm-diameter filter discs (WHA10016508; Merck) for the addition of VOCs (see Supplementary Data 6 & 7). The platform has two black circles with a gap of 20 mm in between; to convert the distance from pixels to cm. Plastic net, nitrile glove, and odorant delivery platform were replaced between repetitions to avoid contamination. Mosquitoes were placed in a 20.3 cm^3 metal cage located in an experimental room with a vent, under a video camera (EOS 70D, lens: MACRO 0.25/0.8 ft; Canon Inc., Tokyo, Japan) and a light ring. Mosquitoes were allowed to acclimate for at least ten minutes before recording. Mosquito behavior was recorded for 10 minutes at 25 frames per second. The number of mosquito detection on the screen and ring were automatically counted using a custom YOLOv11l model. We used the solvent diethyl ether (DEE) as a vehicle. On a blank filter disc, 25 µL of DEE, and DEE with (+)-borneol (1 M, 3.58 mg) were deposited on the filter paper and allowed to evaporate for 2 min prior to mosquito exposure outside the experimental room to avoid contamination. To enhance attractiveness, at the beginning of each experiment, the experimenter first rubbed the ring-mounted glove against the shirt and skin for 1 minute. Additionally, the experimenter blew twice, once into the cage and once into the glove. All experiments were conducted during the first 4 hours of the diurnal period and lasted 10 min. This schedule was chosen for practical reasons and because mosquitoes consistently exhibited attraction to the human hand. Mosquito trajectories were counted and summed for each time interval (30 seconds). We excluded all trajectories that were located more than 2 to 4 mm away from the ring. Statistical comparisons of trajectory visits per time interval were carried out with Mann-Whitney U test (n = 3). For visits variation across repetitions, see Supplementary Fig 12. Statistical comparisons between groups were performed using two-sided Mann–Whitney U tests, and generalized linear mixed models (GLMMs) were fitted in R (v3.6.1; see Supplementary Data 8).

Mosquito detection and software

To investigate the behavioral role of (+)-borneol in mosquitoes, we used YOLito[68]: a YOLOv11l model[69]. We evaluated YOLito on our setup using a test dataset of 180 annotated images (15 images/replicate). YOLito achieved a recall of 0.98, indicating a strong ability to detect true positives, and a precision of 0.86, reflecting accurate identification of mosquitoes. Detections were filtered using a minimum confidence and intersection over union (IoU) threshold of 0.5. All detections are illustrated in Supplementary Fig 12. Model predictions were analyzed with the YOLito toolkit, producing two primary data frames. The first frame contained frame-level data, including frame number, 2D coordinates (x,y), treatment group, and trajectory ID (Source data are provided as a Source Data file). The second frame, summarized behavioral data (Source data are provided as a Source Data file) for each 30 second interval, including (i) cumulative mosquito visits (Fig. 6b), (ii) normalized distance (total distance traveled divided by number of visits, in cm) and (iii) normalized duration (total time spent divided by number of visits, see Source Data file, Supplementary Fig. 11). All custom R code used for statistical analyses is available in the Source Data files.

Statistics & Reproducibility

Except when specifically stated in the figure captions, no data were excluded from the analyses. Unless stated otherwise, the experiments were randomized (e.g., mosquito cohorts were randomly assigned to odor or solvent control, mosquitoes did not experience multiple treatments). The Investigators were blinded to the identity of the composition and formulations of the EOs, sub-mixtures, and single compounds until the final outcome of the functional characterization of OR49.

Reporting summary

Further information on research design is available in the Nature Portfolio Reporting Summary linked to this article.

Data availability

All data supporting the findings of this study are provided within the manuscript and its Supplementary Information. Source data for electrophysiology, calcium imaging, behavioral assays, and phylogenetic analyses are included as accompanying Source Data and Supplementary Data files. No restrictions apply to data availability. Source data are provided with this paper.

Code availability

The R code for statistical analyses (U-test and GLMM) is accessible in the Supplementary Data.

References

1. Wadley, L. et al. Middle stone age bedding construction and settlement patterns at Sibudu, South Africa. *Science* **334**, 1388–1391 (2011).
2. Pålsson, K. & Jaenson, T. G. T. Plant products used as mosquito repellents in Guinea Bissau, West Africa. *Acta Trop.* **72**, 39–52 (1999).
3. Maia, M. F. & Moore, S. J. Plant-based insect repellents: a review of their efficacy, development and testing. *Malar. J.* **10**, S11 (2011).
4. Moore, S. J. & Debboun, M. History of Insect Repellents. In *Insect Repellents: Principles, Methods, and Uses* (eds. Debboun, M., Frances, S. P. & Strickman, D.) vol. 1 (CRC Press, 2007).
5. Kongkaew, C., Sakunrag, I., Chaiyakunapruk, N. & Tawatsin, A. Effectiveness of citronella preparations in preventing mosquito bites: systematic review of controlled laboratory experimental studies. *Trop. Med. Int. Heal.* **16**, 802–810 (2011).
6. Zhu, J. J. et al. Better than DEET repellent compounds derived from coconut oil. *Sci. Rep.* **8**, 14053 (2018).
7. Liu, F. et al. A dual-target molecular mechanism of pyrethrum repellency against mosquitoes. *Nat. Commun.* **12**, 2553 (2021).
8. Iovinella, I., Pelosi, P. & Conti, B. A rationale to design longer lasting mosquito repellents. *Parasitol. Res.* **113**, 1813–1820 (2014).
9. Poudel, D. K. et al. The chemical profiling of essential oils from different tissues of *Cinnamomum camphora* L. and their antimicrobial activities. *Molecules* **26**, 5132 (2021).
10. Mei, Y. et al. The history, stereochemistry, ethnopharmacology and quality assessment of borneol. *J. Ethnopharmacol.* **300**, 115697 (2023).

11. Erdelyan, C., Mahood, T., Bader, T. & Whyard, S. Functional validation of the carbon dioxide receptor genes in *Aedes aegypti* mosquitoes using RNA interference. *Insect Mol. Biol.* **21**, 119–127 (2012).
12. McMeniman, C. J., Corfas, R. A., Matthews, B. J., Ritchie, S. A. & Vosshall, L. B. Multimodal integration of carbon dioxide and other sensory cues drives mosquito attraction to humans. *Cell* **156**, 1060–1071 (2014).
13. Lu, T. et al. Odor coding in the maxillary palp of the malaria vector mosquito *Anopheles gambiae*. *Curr. Biol.* **17**, 1533–1544 (2007).
14. Grant, A. J. & Dickens, J. C. Functional characterization of the octenol receptor neuron on the maxillary palps of the yellow fever mosquito, *Aedes aegypti*. *PLoS ONE* **6**, e21785 (2011).
15. Grant, A. J. & O'Connell, R. J. Electrophysiological responses from receptor neurons in mosquito maxillary palp sensilla. in (ed. Block, E.) vol. 200 233-48-discussion 248-53-281–4 (John Wiley & Sons, Ltd., 1996).
16. Takken, W. & Kline, D. L. Carbon dioxide and 1-octen-3-ol as mosquito attractants. *J. Am. Mosq. Control Assoc.* **5**, 311–316 (1989).
17. Gillies, M. T. The role of carbon dioxide in host-finding by mosquitoes (Diptera: Culicidae): a review. *Bull. Entomol. Res.* **70**, 525–532 (1980).
18. Wang, G., Carey, A. F., Carlson, J. R. & Zwiebel, L. J. Molecular basis of odor coding in the malaria vector mosquito Anopheles gambiae. *PNAS* **107**, (2010).
19. Bohbot, J. et al. Molecular characterization of the *Aedes aegypti* odorant receptor gene family. *Insect Mol. Biol.* **16**, 525–537 (2007).
20. Matthews, B. J. et al. Improved reference genome of *Aedes aegypti* informs arbovirus vector control. *Nature* **563**, 501–507 (2018).
21. Bohbot, J. D. & Dickens, J. C. Characterization of an enantioselective odorant receptor in the yellow fever mosquito *Aedes aegypti*. *PLoS ONE* **4**, e7032 (2009).
22. Majeed, S., Hill, S. R., Dekker, T. & Ignell, R. Detection and perception of generic host volatiles by mosquitoes: responses to CO2 constrains host-seeking behaviour. *R. Soc. open Sci.* **4**, 170189 (2017).
23. Majeed, S., Hill, S. R., Birgersson, G. & Ignell, R. Detection and perception of generic host volatiles by mosquitoes modulate host preference: context dependence of (R)–1-octen-3-ol. *R. Soc. open Sci.* **3**, 160467 (2016).
24. Bohbot, J. D., Durand, N. F., Vinyard, B. T. & Dickens, J. C. Functional development of the octenol response in *Aedes aegypti*. *Front. Physiol.* **4**, 39 (2013).
25. Zhao, Z., Tian, D. & McBride, C. S. Development of a pan-neuronal genetic driver in *Aedes aegypti* mosquitoes. *Cell Rep. Methods* **1**, 100042 (2021).
26. Lahondère, C. et al. The olfactory basis of orchid pollination by mosquitoes. *Proc. Natl. Acad. Sci. USA*. (2019) https://doi.org/10.1073/pnas.1910589117.
27. Shankar, S. & McMeniman, C. J. An updated antennal lobe atlas for the yellow fever mosquito *Aedes aegypti*. *Plos Negl. Trop. D.* **14**, e0008729 (2020).
28. Wolff, G. H., Lahondère, C., Vinauger, C., Rylance, E. & Riffell, J. A. Neuromodulation and differential learning across mosquito species. *Proc. R. Soc. B* **290**, 20222118 (2023).
29. Anton, Loon, S., van, J., Meijerink, J. & Smid, H. Central projections of olfactory receptor neurons from single antennal and palpal sensilla in mosquitoes. *Arthropod Struct. Dev.* **32**, 319–327 (2003).
30. Cloyd, R. A., Marley, K. A., Larson, R. A., Dickinson, A. & Arieli, B. Repellency of naturally occurring volatile alcohols to fungus gnat *Bradysia* sp. nr. *coprophila* (Diptera: Sciaridae) adults under laboratory conditions. *J. Econ. Entomol.* **104**, 1633–1639 (2011).
31. Liang, Y. et al. Evaluation of repellency of some chinese medicinal herbs essential oils against *Liposcelis bostrychophila* (Psocoptera: Liposcelidae) and *Tribolium castaneum* (Coleoptera: Tenebrionidae). *J. Econ. Entomol.* **106**, 513–519 (2013).
32. Zhang, N. et al. Insecticidal, Fumigant, and Repellent Activities of Sweet Wormwood Oil and Its Individual Components Against Red Imported Fire Ant Workers (Hymenoptera: Formicidae). *J. Insect Sci.* **14**, 241 (2014).
33. Wood, M. J., Bull, J. C., Kanagachandran, K. & Butt, T. M. Development and laboratory validation of a plant-derived repellent blend, effective against *Aedes aegypti* [Diptera: Culicidae], Anopheles gambiae [Diptera: Culicidae] and Culex quinquefasciatus [Diptera: Culicidae]. *PLOS ONE* **19**, e0299144 (2024).
34. Hill, C. A. et al. G protein-coupled receptors in Anopheles gambiae. *Science* **298**, 176–178 (2002).
35. Carey, A. F., Wang, G., Su, C.-Y., Zwiebel, L. J. & Carlson, J. R. Odorant reception in the malaria mosquito Anopheles gambiae. *Nature* **464**, 66–71 (2010).
36. Bohbot, J. D. & Pitts, R. J. The narrowing olfactory landscape of insect odorant receptors. *Front. Ecol. Evol.* **3**, 39 (2015).
37. Hwang, Y.-S., Wu, K.-H., Kumamoto, J., Axelrod, H. & Mulla, M. S. Isolation and identification of mosquito repellents in Artemisia vulgaris. *J. Chem. Ecol.* **11**, 1297–1306 (1985).
38. Pitarokili, D., Michaelakis, A., Koliopoulos, G., Giatropoulos, A. & Tzakou, O. Chemical composition, larvicidal evaluation, and adult repellency of endemic Greek Thymus essential oils against the mosquito vector of West Nile virus. *Parasitol. Res.* **109**, 425–430 (2011).
39. Waliwitiya, R., Kennedy, C. J. & Lowenberger, C. A. Larvicidal and oviposition-altering activity of monoterpenoids, trans-anithole and rosemary oil to the yellow fever mosquito *Aedes aegypti* (Diptera: Culicidae). *Pest Manag Sci.* **65**, 241–248 (2009).
40. Picollo, M. I., Toloza, A. C., Cueto, G. M., Zygadlo, J. & Zerba, E. Anticholinesterase and pediculicidal activities of monoterpenoids. *Fitoterapia* **79**, 271–278 (2008).
41. Abdelgaleil, S. A. M., Mohamed, M. I. E., Badawy, M. E. I. & El-arami, S. A. A. Fumigant and Contact Toxicities of Monoterpenes to Sitophilus oryzae (L.) and *Tribolium castaneum* (Herbst) and their Inhibitory Effects on Acetylcholinesterase Activity. *J. Chem. Ecol.* **35**, 518–525 (2009).
42. Rajkumar, S. & Jebanesan, A. Chemical composition and larvicidal activity of leaf essential oil from Clausena dentata (Willd) M. Roam. (Rutaceae) against the chikungunya vector, *Aedes aegypti* Linn. (Diptera: Culicidae). *J. Asia-pac. Entomol.* **13**, 107–109 (2010).
43. Afify, A. & Galizia, C. G. Gravid females of the mosquito *Aedes aegypti* avoid oviposition on m-cresol in the presence of the deterrent isomer p-cresol. *Parasite Vector* **7**, 315 (2014).
44. Raj, G. A., Chandrasekaran, M., Krishnamoorthy, S., Jayaraman, M. & Venkatesalu, V. Phytochemical profile and larvicidal properties of seed essential oil from Nigella sativa L. (Ranunculaceae), against *Aedes aegypti*, Anopheles stephensi, and Culex quinquefasciatus (Diptera: Culicidae). *Parasitol. Res.* **114**, 3385–3391 (2015).
45. Nunes, R. K. V. et al. Evaluation of (–)-borneol derivatives against the Zika vector, *Aedes aegypti* and a non-target species, Artemia sp. *Environ. Sci. Pollut. R.* **25**, 31165–31174 (2018).
46. Ignell, R., Dekker, T., Ghaninia, M. & Hansson, B. S. Neuronal architecture of the mosquito deutocerebrum. *J. Comp. Neurol.* **493**, 207–240 (2005).

47. Ng, R., Wu, S. & Su, C. Neuronal Compartmentalization: A Means to Integrate Sensory Input at the Earliest Stage of Information Processing? *Bioessays* **42**, e2000026 (2020).
48. Dekel, A., Sar-Shalom, E., Vainer, Y., Yakir, E. & Bohbot, J. D. The oviposition cue indole inhibits animal host attraction in *Aedes aegypti* (Diptera: Culicidae) mosquitoes. *Parasite Vector* **15**, 422 (2022).
49. Zhou, X., Rinker, D. C., Pitts, R. J., Rokas, A. & Zwiebel, L. J. Divergent and conserved elements comprise the chemoreceptive repertoire of the non-blood feeding mosquito Toxorhynchites amboinensis. *Genome Biol. Evol.* **6**, 2883–2896 (2014).
50. Chenna, R. et al. Multiple sequence alignment with the Clustal series of programs. *Nucleic Acids Res.* **31**, 3497–3500 (2003).
51. Kearse, M. et al. Geneious Basic: An integrated and extendable desktop software platform for the organization and analysis of sequence data. *Bioinformatics* **28**, 1647–1649 (2012).
52. Palatini, U. et al. Improved reference genome of the arboviral vector Aedes albopictus. *Genome Biol.* **21**, 215 (2020).
53. Boyle, J. H. et al. A Linkage-Based Genome Assembly for the Mosquito Aedes albopictus and Identification of Chromosomal Regions Affecting Diapause. *Insects* **12**, 167 (2021).
54. Arensburger, P., Hice, R. H., Wright, J. A., Craig, N. L. & Atkinson, P. W. The mosquito *Aedes aegypti* has a large genome size and high transposable element load but contains a low proportion of transposon-specific piRNAs. *BMC Genom.* **12**, 606–606 (2011).
55. Sharakhova, M. V. et al. Update of the Anopheles gambiaePEST genome assembly. *Genome Biol.* **8**, R5 (2007).
56. Dekel, A., Pitts, R. J., Yakir, E. & Bohbot, J. D. Evolutionarily conserved odorant receptor function questions ecological context of octenol role in mosquitoes. *Sci. Rep.* **6**, 37330 (2016).
57. Huff, R. M. & Pitts, R. J. Carboxylic acid responses by a conserved odorant receptor in culicine vector mosquitoes. *Insect Mol. Biol.* **29**, 523–530 (2020).
58. Wang, Y. et al. Molecular basis of peripheral olfactory sensing during oviposition in the behavior of the parasitic wasp Anastatus japonicus. *Insect Biochem. Mol. Biol.* **89**, 58–70 (2017).
59. Herre, M. et al. Non-canonical odor coding in the mosquito. *Cell* **185**, 3104–3123.e28 (2022).
60. Ghaninia, M., Majeed, S., Dekker, T., Hill, S. R. & Ignell, R. Hold your breath – Differential behavioral and sensory acuity of mosquitoes to acetone and carbon dioxide. *Plos One* **14**, e0226815 (2019).
61. Syed, Z. & Leal, W. S. Maxillary palps are broad spectrum odorant detectors in Culex quinquefasciatus. *Chem. Senses* **32**, 727–738 (2007).
62. Cook, J. I. et al. Enantiomeric selectivity in behavioural and electrophysiological responses of *Aedes aegypti* and Culex quinquefasciatus mosquitoes. *Bull. Entomol. Res.* **101**, 541–550 (2011).
63. Omondi, B. A., Majeed, S. & Ignell, R. Functional development of carbon dioxide detection in the maxillary palp of Anopheles gambiae. *J. Exp. Biol.* **218**, 2482–2488 (2015).
64. Singh, S. S. et al. Plasticity and interactions in the odor responses of maxillary palps neurons in *Aedes aegypti*. *bioRxiv* 2022.10.02.510498 (2022) https://doi.org/10.1101/2022.10.02.510498.
65. Bruyne, M. de, Foster, K. & Carlson, J. Odor coding in the Drosophila antenna. *Neuron* **30**, 537–552 (2001).
66. Melo, N. et al. Geosmin attracts *Aedes aegypti* mosquitoes to oviposition sites. *Curr. Biol.* **30**, 1–8 (2020).
67. Vinauger, C. et al. Visual-Olfactory Integration in the Human Disease Vector Mosquito *Aedes aegypti*. *Curr. Biol.* **29**, 2509–2516.e5 (2019).
68. Sar-Shalom, E. et al. YOLito: A generalizable model for automated mosquito detection. *bioRxiv: Prepr. Serv. Biol.* 2025.11.20.689454 (2025) https://doi.org/10.1101/2025.11.20.689454.
69. Jocher, G., Chaurasia, A. & Qiu, J. YOLO by Ultralytics (Version 8.0.0)[Computer software]. (2023).

Acknowledgements

This study was supported by ISF 997/19 awarded to A.W., ISF 719/21 and MOST 0005666 awarded to J.D.B., NIH R01AI175152 and NSF IOS-2242604 awarded to O.S.A., NIAID R01AI148300 awarded to J.A.R, O.S.A., and R.J.P. J.A.R was funded by the Bill and Melinda Gates Foundation (INV-021766). National Key Research and Development Program (2023YFE0113600) awarded to Y.W. This research was supported by the Ministry of Science & Technology, Israel to P.A.P. (grant numbers 3-16795 and 3-17985). We thank Ziv Kassner for consultation, processing, analysis guidance, and technical support in the creation of the mosquito detection model. We are especially grateful to Nadav Eyal at Eybna Terpene Based Technologies for their time and supply of *Cannabis* essential oils. We are grateful to Dr. Laor Orshan (Ministry of Health, Israel) for providing a colony of *Culex pipiens*. Special thanks to Dr. Osnat Malka for productive discussions. Drs. Pitts and Bohbot are co-corresponding authors.

Author contributions

J.D.B. conceived and led the study. R.J.P. initiated the deorphanization of OR49 and contributed to the concept of the study. R.J.P. and R.M.H. initiated the functional characterization of OR49. Y.V. identified borneol as a key OR49 ligand. E.S.S. conducted the behavioral experiments, created the YOLito model, and analyzed the data. Y.W. conducted mosquito electropalpograms. R.M.H. identified camphor as an OR49 agonist. O.S.A. and I.V.C.-A. engineered the *Ae. aegypti Or49* knockout strain. M.G. and R.I. designed and conducted the single sensillum recordings. D.P. and P.A.P. conducted gene annotations, phylogenetic analyses, and described *Or49* syntenic relationships. D.R. completed the *Toxorhynchites amboinensis Or* genomic PCRs and sequencing. C.R. and J.A.R. conducted brain imaging. E.Y. provided genetic constructs and injectable mRNA. A.W. provided funding and scientific oversight. J.D.B. wrote the manuscript with individual contributions from all the authors.

Competing interests

O.S.A is a founder of Agragene, Inc. and Synvect, Inc. with equity interest. The terms of this arrangement have been reviewed and approved by the University of California, San Diego, in accordance with its conflict-of-interest policies. All other authors declare no competing interests.

Additional information

Supplementary information The online version contains supplementary material available at https://doi.org/10.1038/s41467-026-69511-z.

Correspondence and requests for materials should be addressed to Ronald Jason Pitts or Jonathan D. Bohbot.

Peer review information *Nature Communications* thanks the anonymous reviewer(s) for their contribution to the peer review of this work. A peer review file is available.